Trans Indian Inst Met (2019) 72(7):1765–1774
https://doi.org/10.1007/s12666-019-01647-7

TECHNICAL PAPER

Microstructural, Tribological and Mechanical Properties Evolution of $ZrSiO_4$/A4047 Surface Composite Fabricated through Friction Stir Processing

Surendra Kumar Patel[1] · Virendra Pratap Singh[1] · Basil Kuriachen[1]

Received: 4 November 2018 / Accepted: 26 February 2019 / Published online: 22 March 2019

Abstract In this study, zircon sand ($ZrSiO_4$)-reinforced aluminum surface composite up to 15 vol % of microparticles with an average diameter of 3 μm was prepared through multi-pass FSP. The microstructural, mechanical and tribological characterizations of the friction stir-processed $ZrSiO_4$/A4047 surface composite were evaluated. The effects of FSP passes (2, 4 and 6) were evaluated, and it suggests that the surface composite after 6-pass reveals better homogeneous distribution of reinforcement ($ZrSiO_4$) particle in the matrix. The tensile test showed 16, 24 and 44% with increase in FSP passes, respectively, compared to the base metal. Similarly, the microhardness of the surface composite produced through 6-pass FSP was increased to 112 HV while that produced through base metal increased to 74 HV. Also, it was observed that erosion–corrosion resistance and abrasion wear performance were significantly improved with increase in FSP passes.

Keywords A4047 alloys · Zircon particles · Friction stir processing · Surface composite · Wear

1 Introduction

In the present era, aluminum and its alloys are being used in the aerospace, marine automobile and many other industrial and commercial parts due to their improved materials properties [1]. This is due to fact that they exhibit excellent strength to weight fraction and are easily weldable due to plastic formability and strengthening. However, in some of the applications, the aluminum and its alloy are not suitable due to lack of tribological performance and mechanical properties. Therefore, researchers have mixed various reinforcement particles to improve the mechanical properties [2–4]. Reinforced aluminum matrix composites with carbide/ceramics particles has not only improved the mechanical properties, but has also resulted in improvement of specific wear rate, friction coefficient [5] and tribological properties [6, 7]. It has also been found from the literature that, many processes have been used to produce the bulk aluminum matrix composites (referred as AMCs). However, surface engineering has a wide range of applications to modify/reinforce the surface properties of the material via retaining the bulk material properties. Among the available well-established surface modification techniques [8], surface modification through severe plastic deformation (referred as SPD) is an effective method for producing ultrafine-grained material coatings [9]. Even though there are many well-established SPD techniques, SPD by friction stir processing (FSP) can be utilized to improve the grain refinement, surface hardness and also the tribological features of aluminum alloys [10]. The FSP is a newly developed method to produce an intermetallic surface layer through the formation of ultrafine and equiaxed grains by recrystallization, which is initiated by frictional heating [11]. It has also been found that mechanical properties are enhanced significantly due to the enhancement of grain size. Various researchers have tried various methodologies to improve the properties of aluminum alloys through FSP. A few have analyzed the single reinforcements such as A356/B_4C [12], A1050/Nb [13], A6061/TiB_2 [14], AZ-31/Ni [15], A6083/Mo [16], AZ-31/Si [17] and AZ-31/ZrO_2 [18]. On the other hand, hybrid surface composites develop with dual reinforcement

✉ Basil Kuriachen
basilkuriachen@gmail.com

[1] Department of Mechanical Engineering, National Institute of Technology Mizoram, Aizawl, Mizoram 796012, India

Table 1 Elemental composition of A4047

Alloy	Si	Fe	Cu	Zn	Mn	Mg	Be	Balance
A4047 (wt %)	11–13	0.8	0.3	0.2	0.15	0.1	0.0008	Al

particles like A8026/TiB_2–Al_2O_3 [19], A5083/Al_2O_3–TiO_2 [20], A413/SiC–MoS_2 [21], A6061/Al_2O_3–TiB_2 [22] and A356/SiO_2–Al_2O_3 [23]. Moreover, the scientific communities are also focusing on advanced composite/ceramics/alloys/solid solution due to their possible promising applications [24–28]. Among various reinforcement particles, zircon sand-reinforced composite seem to have high thermal and refractoriness [29–31], excellent erosion–corrosion resistance to chemical attack and typical wear resistance compared to other reinforced particles into Al metal matrix. Therefore, an effort has been made to develop a zircon sand-reinforced aluminum surface composite through FSP and instigate the microstructural, mechanical and tribological behavior.

2 Experimental Methods

In this study, a commercially available A4047 aluminum plate of 6 mm thickness with the elementary fraction are shown in Table 1. The zircon sand with average size of 3 μm as shown in Fig. 1, was used as reinforcement particles. The zircon sand was filled into a groove of 3 mm width and 3 mm depth on the aluminum plate. To produce the surface composite of 15 vol %, zircon particles were placed and covered through a pin-less tool. In order to process the FSP, tungsten carbide tool with a shoulder diameter of 20 mm and tapped pin with a length of 5 mm was selected. The fabrication of surface composite was performed with an optimized process parameters such as tool rotation of 1200 rpm, traverse speed of 40 (mm/min) and a tool tilt angle of 3°. In order to study the effects of the number of FSP passes on the uniform distribution, microstructure, mechanical and tribological properties, samples with 2, 4 and 6 FSP passes were developed with 100% overlap. The microstructural analysis and uniform distribution of developed surface composites were performed using scanning electron microscopy (SEM). All the samples were mechanically polished with abrasive SiC sandpaper, followed by polishing using alumina paste. Polished samples (without disturbed layer) revealed porosity, cracks, presence of graphite flakes in aluminum alloy, etc., but suitable etching solution was necessary to witness the different phases noticeable under a typical metallurgical microscope [14–19]. Further, specimens for the tensile test were cut from the stir zone as per the ASTM standard of E8/E8 M-11. Microhardness and wear resistance of the fabricated surface composite were analyzed. Microhardness tester (Model: VMHT 30A) and abrasion tester (TR-44) were used for experimentation with a solution containing 5% sodium chloride, 20% fine silica sand and 75% tap water, respectively. All the samples were cleaned by acetone before characterization.

3 Results and Discussion

3.1 Microstructural Analysis

Morphological and microstructural features of the composites are shown in Fig. 2. The composite sample has been exposed to 2, 4 and 6 passes, separately as revealed in Fig. 2a–c. Figure 2d shows the grain refinement measurement of the reinforced particles after 6-pass FSP. Surface micrograph indicates the improved flow of materials due to ultragrain refinement of particles in stir zone during FSP. The microstructure of fabricated composites in broken areas is fundamentally the same as grain estimate list. The grains at the specimen's cross section, display some allowance because of the action of the moving plate. The microstructure of FSPed composite demonstrates a few kinds of second-stage particles consistently circulated in the matrix and arranged along the movement. Three essential kinds of intermetallic atoms are found in the fabricated matrix. Figure 3a–d demonstrate the morphology of the strong Al_2O_3 particles present in the considered combination. The network of Al_2O_3 particles (Fig 3d), are adjusted and others present a further quadrangular morphology. The more bounteous particles are those that contain the Al–Si stoichiometric phase. These atoms present distinctive size and shapes, as it can be seen in Fig. 3b.

The microstructural aspects of the A4047 with $ZrSiO_4$ particles as reinforcement in metal matrix composite has been externally examined. The investigation included estimation of average FSP deformities and material reaction under the connected loads and heat input. All the $ZrSiO_4$-reinforced metal matrix surface composites (MMSCs) demonstrate a decent appearance, very much twisted with no visible deformities. No particle collection can be seen on their surface. A longitudinal deformity is on the propelling side, and a molecule assumption is on the withdrawing side [32]. Inside and outside of the $ZrSiO_4$ powder reinforced MMSCs are revealed by cutting along the transverse direction, and samples are examined by SEM. It is clarified that on the surface, the fortifying particles are lost amid the procedure as they stay implanted in the burrs produced in each pass. It is clear from the SEM micrographs that the $ZrSiO_4$ particles are divided as an outcome of the mixing of tool. Because of this procedure, a

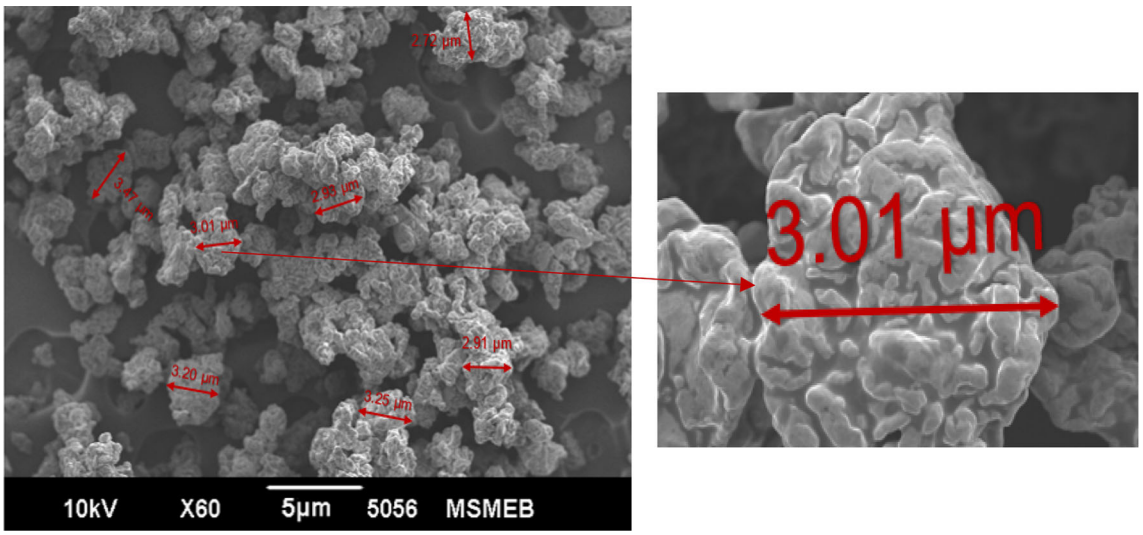

Fig. 1 Grain measurement of zircon particles

higher number of settled particles of smaller sizes are seen in the SZ.

The FSP plays an important role in grain refinement/modification of surface properties through clustering and several plastic deformation developments between the atoms into stir zone. The 2-pass surface composite displays the lowest grain refinement which is shown in Fig. 3b, whereas the 6-pass composites display more ultragrained particles sizes which is shown in Fig. 3d. The morphology and dispersion of $ZrSiO_4$ particles into the stir zone are examined through scanning electron microscopy (SEM). Micrographs reveal that the strengthening particles are properly incorporated into matrix through the FSP passes. As revealed, the widespread cluster of the strengthening particles ($ZrSiO_4$) is shown in 2-pass surface composite. The better dispersion of reinforced particles over the surface happens due to the development of frictional heat between tool and workpiece [33]. Yet, increasing the FSP passes gives a better uniform spreading of ($ZrSiO_4$) particles due to the effect of the reheating and recrystallization between stirred molecules.

3.2 Tensile Features

The mechanical tensile strength is represented through stress–strain curves, for numerous fabricated composites (e.g., 2, 4 and 6), as shown in Fig. 4. With increasing FSPed passes, modified composites have been subjected to better tensile properties. The ultimate tensile strength of fabricated surface composites get progressively improved with increasing number of passes (e.g., 2, 4 and 6 passes). Friction stirred samples show an enhancement in the tensile strength and yield. According to the Hall–Petch relationship, the reinforcement particle refinement of the composites (in stir zone) is moderately effective in enhancing the mechanical properties, like as tensile strength and microhardness [34]. The metallo-graphic examination reveals an increase in contact area of the reinforced particle between the matrix surface composite. Due to increasing the contact area, the tensile sample shows a dimpled structure in the surface of the matrix. Due to the slight depression of reinforcement in a surface, the atom arrays increases in the stir zone. Thus, in the refinement of microstructure during FSP, the yield and ultimate tensile strength increase.

The rupture features of the tensile samples are compared to the rupture characteristics of FSPed samples. The microstructure behavior of the fissure surface is analyzed through SEM. The SEM microimage (micrographs) of distinguished samples are shown in Fig. 5a–d. Hence, due to a ductile failure, the rupture surface of the samples present a dented structure. The occurrence of large number of warped pits specified as plastic deformation earlier to failure, involvement of better distorted lemon structure depressions over the surface, the fracture features of (6-pass) FSPed composite specify an effective plastic distortion earlier to fracture in micrograph. This is a better promise that with the outcomes of tensile examination, which is shown in Fig. 4, composites that are imperiled to multi-number of FSPed passes show an increased percentage of elongation earlier to fracture. Still, elastic behavior of the base metal is shown to be greater than the 2-pass developed composite. This can be credited to widespread cluster and heterogeneous distribution of reinforcement (zircon sand) particles in the 2-pass surface composite sample.

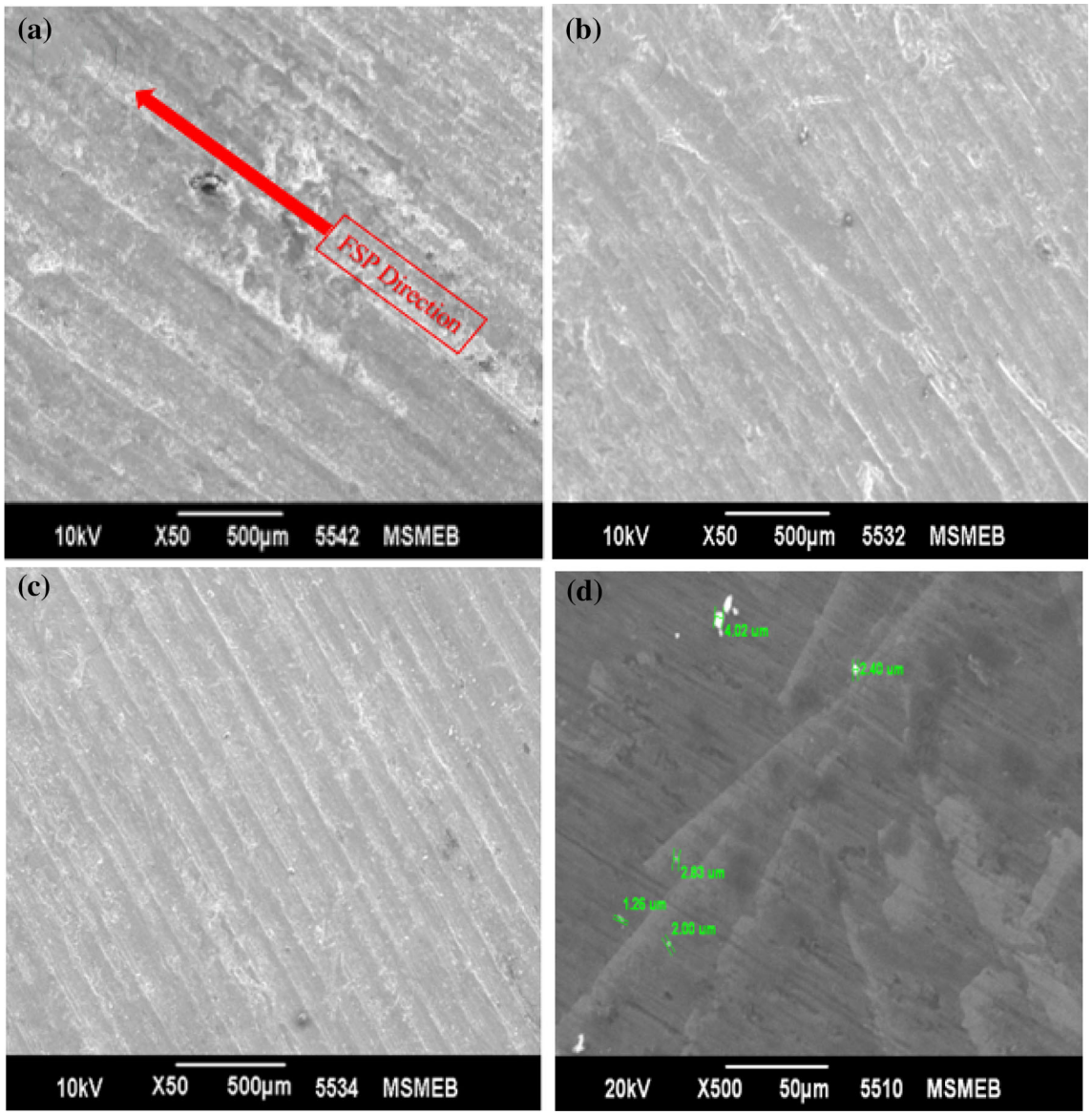

Fig. 2 SEM micrograph of developed surface composite after **a** 2 pass, **b** 4 pass, **c** 6 pass and **d** grain refinement measurement after 6 pass

The large amount of reinforcement particles clusters at 2-pass FSP, so that the developed surface composite performance such as the beginning of defects can be found to reduce the tensile strength. Alternatively, a further equal distribution of the reinforcement grains into the matrix rebounds and prevents the progress of more propagation of cracks to improve the mechanical characteristic of the surface composites [35–37]. Also, the presence of more holes (porosity) may be observed during the fabrication time by FSP into the surface composites. Porosity may develop in surface composites owing to the admission of reinforcement ($ZrSiO_4$) particles. The density measurement is subjected to equate the porosity fraction of the composite.

3.3 Density Measurement

The density observation has been completed with the Archimedes principle. The density value of numerous developed composites is shown in Table 2. In Table 2, the 2-pass FSPed composite has the highest density due to well distributed fine sized pores. The SEM micrograph of stir zone of the (2-, 4- and 6-pass) composite are shown in Fig. 3. The mixing of reinforced particles effective in the development of huge porosity (absorbency) can promote a poor tensile strength and a lower elongation (deformation) before rupture.

As it is revealed, increasing number of FSP passes result in enhanced dispersion of reinforcement (zircon sand) particles. Even, 4- and 6-pass composites have nearly equal

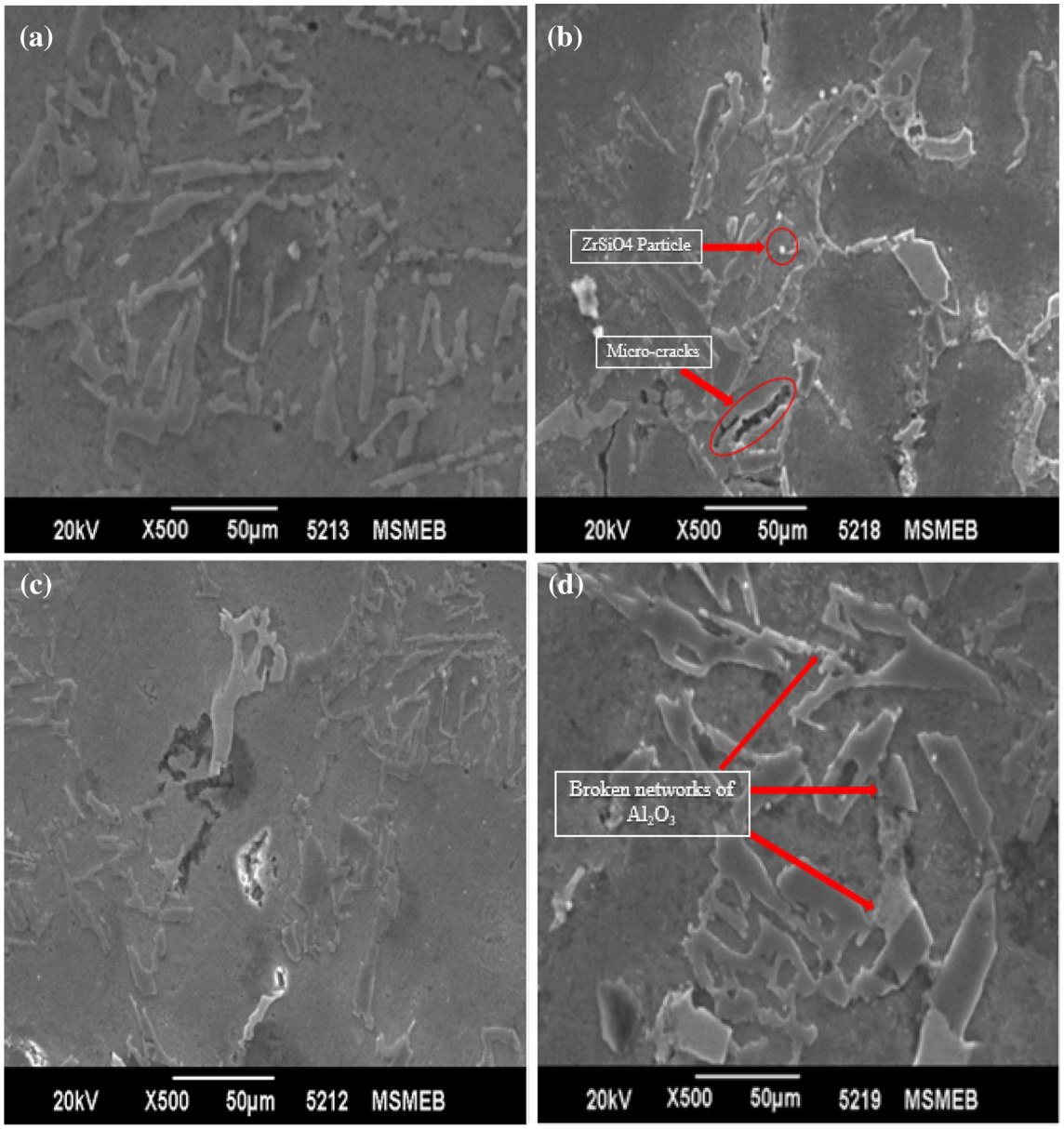

Fig. 3 SEM micrographs **a** base metal and distribution of the zircon sand particles after **b** 2 pass, **c** 4 pass and **d** 6 pass

values of density, and the 6-pass composite displays a greater strength, but a poor elongation earlier to fracture as compared to 2 and 4 passes. Increasing the processing passes from 2 to 6 control the enhancement of tensile strength and fraction of elongation earlier to fracture. This is credited to the synchronized growth of the sample's strain hardening and density. In a different region, though increasing number of the passes may not have, modified the density meaningfully, but as the number passes increase intensely, superior tensile strengths with lower elongation to fracture is observed for the 6-pass composite. Hence, increasing the FSPed passes from 2 to 6 increases the composites density, due to more uniform distribution of reinforcement ($ZrSiO_4$) particles, which are associated with more tensile strength and elongation earlier to rupture. It is supposed that an equiaxed and ultrafine grain microstructure of the composite along with unvaryingly dispersed satisfactorly reinforced particles can afford equal distortion and improved ductility to FSPed composites.

3.4 Microhardness Measurement

The microhardness profile is followed in 1 mm depth and spacing. The best surface is from AS to RS, producing 1 mm equidistant focuses and its equivalent. The microhardness in few areas decreases because of molecule-free

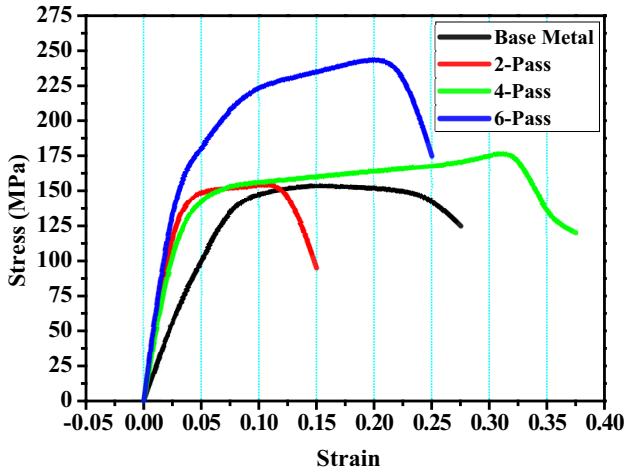

Fig. 4 Stress–strain curves of the base metal and friction stirred (2-, 4- and 6-pass) sample

locale and it demonstrates an extremely scattered profile because of inhomogeneous molecular circulation [38]. It is to be noticed that in spite of the fact that the expansion in number of passes results in more homogeneous dispersion of molecule and more prominent grain refinement, the hardness has not expanded by a practically identical sum [39]. The A4047 aluminum contains significant amount of magnesium silicide and this is the principle explanation behind its high quality. In A4047 amalgams, expansion of each FSP pass likewise increments related warmth info and causes coagulation and decrease in accelerated thickness or even the disintegration of hastens, and thus, may cause drop in hardness. The expansion in normal hardness with expanding passes is proportionately less in contrast with the gain because of partner refinement and level of homogenization. This drop may be credited to coagulation and decrease in precipitation thickness. A similar perception may be deduced from the microhardness measurement. In the present case, the impact of coagulation, sparsing of dissemination and disintegration of hastens are most likely more than the impact of $ZrSiO_4$ particles. In any case, the hardness of surface composites increment with expanding FSP passes and the pinnacle hardness of the considerable number of tests is higher, which may be credited to the homogeneous and better scattering of $ZrSiO_4$ particles in the matrix. Besides, the outcomes exhibit the noteworthy impact of quantities of passes on the molecule scattering and deformity development in the manufacture of surface composites.

The influence of processing on the mechanical properties of composites has been studied through microhardness evolution. The microhardness values of modified composites are achieved along with processing zone. Measurements are completed by loading time of 10 s at 20 N load. The microhardness values on the stir zone of each sample are shown in Fig. 6, and the microhardness values that has been testified in this examination are the average values of at least five values of composites (91.82%). The microhardness of base metal is near 74 (HV), while the microhardness in stir zone of the 6-pass composite is approximately 112 HV. Also, the equal dispersion of zircon sand into the stirred zone (SZ) is measured to be comparatively uniform which designates an equal deformation and the effectual dispersion of the reinforcement ($ZrSiO_4$) zircon sand particles into developed composites. The better microhardness of modified surface composites may be achieved due to the occurrence of zircon sand ($ZrSiO_4$) particles. In addition, microhardness of modified composite improves as the FSPed passes increases. The increase in processing passes achieve a better microhardness of composite through a more equal distribution of reinforcement, as well as the deformed matrix particle of base metal. The large silicon content in Al alloy (A4047) promotes solid result, increasing mechanical strength and the fluidity into the matrix [40].

The correlation of smaller-scale hardness on the diverse zones of the prepared examples show that the hardness value is higher in the SZ and continuously decreases toward the HAZ. The improvement in hardness esteems in the SZ may be ascribed to various reinforcing components. According to the fortifying component, zircon sand ($ZrSiO_4$) powder particles scattered in SZ impede disengagement movement, and along these lines, plastic disfigurement is caused by space. According to the shear slack system, the heap is exchanged from the network to aluminum oxide through interfacial shear. This shear pressure upsets disengagement movement and the plastic distortion [41, 42]. The substantial contrast among the heat coefficient of the substrate and reinforcing powder results in an expansion of disengagements at the interface prompting solidification of the lattice. However, reinforcement and grain refinement stimulation are found to mostly adept in clarifying the higher hardness value in the SZ. Decrease in hardness value in the HAZ is the consequence of grains development and disintegration/coarsening of accelerated particles developed through sluggish cooling rate. Even so, microhardness in thermal zone increases when compared with HAZ, which may be credited to moderately fine grains and work solidifying component.

3.5 Wear Analysis

Figure 7a–d shows the abrasive wear curves of the friction stirred composites and base metal. The weight loss measurements' outcome for individual sample is shown in Table 3. As is observed since ($ZrSiO_4$) strengthening elements are like binding materials into the Al matrix, the wear performance of 6-pass composite is more positive

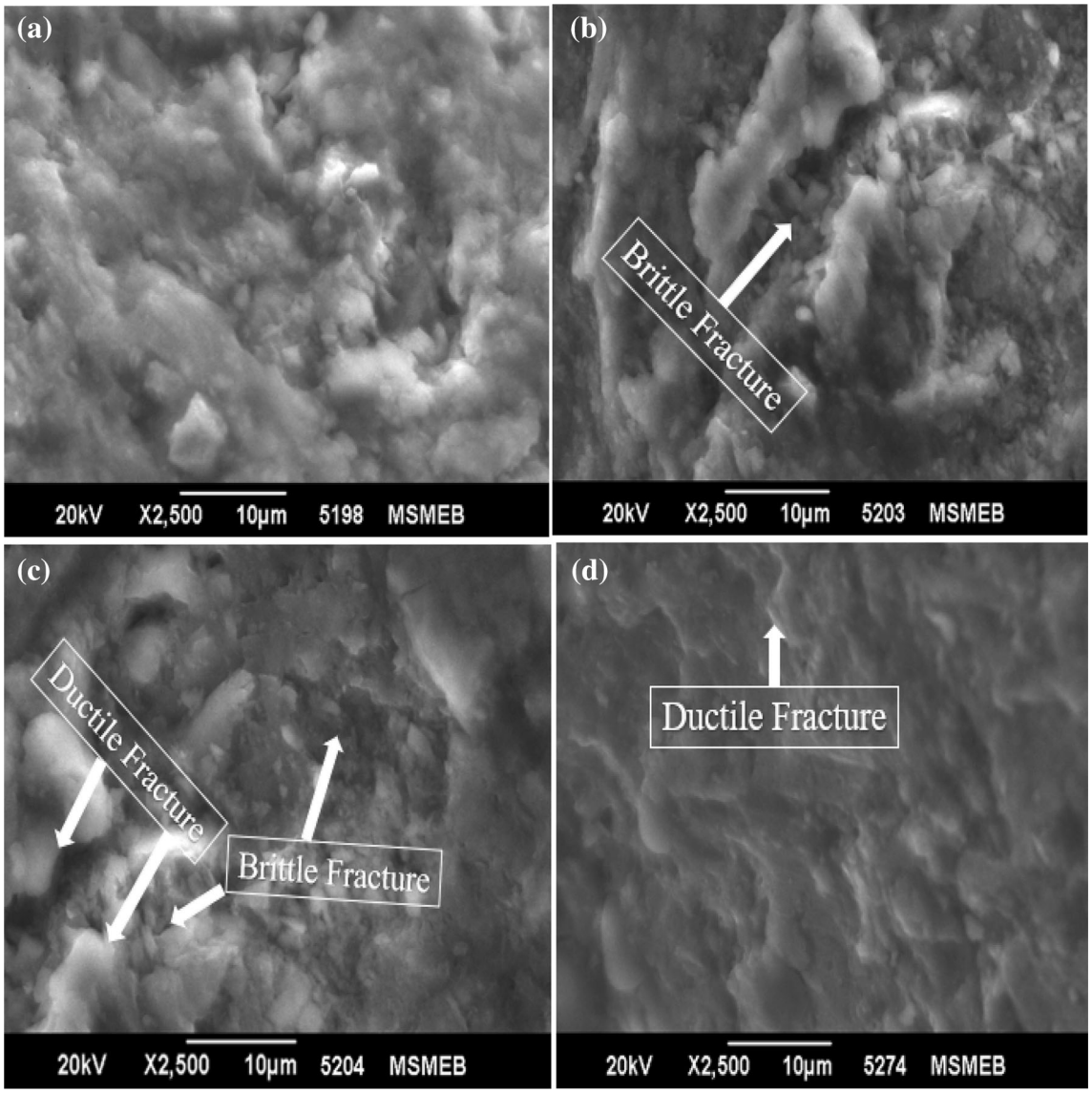

Fig. 5 SEM fractographs of **a** base metal, friction stirred sample after **b** 2-pass **c** 4-pass and **d** 6-pass composites

Table 2 Density measurement of base metal and fabricated surface composite

Sample	Base metal	2 pass	4 pass	6 pass
Density (g/cm^3)	2.6	2.71	2.65	2.63

than 4-pass, 2-pass and base metal composite. Also, increasing the number of FSP pass results in reducing the wear rate [43]. This may have resulted from the operative formation of grain's limitations, which lead to the grain's modification during the FSPed passes. Grains impose restrictions and further deformation results in structural imperfections in the Al-matrix. Also, increasing the FSP passes increases the deepness of penetration of strengthening particles and increases the grain refinement of particles over the fabricated surface layer [44]. Because of ($ZrSiO_4$) strengthening particles into the Al matrix, reducing the strengthening particle on the surface moves the better wear resistance to further lower wt. loss values.

Additionally, the wear behavior of fabricated composite is severely affected by the number of FSP pass with the existence of reinforcement particles [45]. While the base metal and 2-pass sample display a lower wear resistance, the 6-pass reinforced composite shows a better wear resistance as compared to another modified surface composite (such as 2 and 4 passes). The presence of bulk agglomerates of strengthening particles and apertures in the 2-pass composites generate large gaps in the surface oxide film and improves the wear resistance over the composite surface. Still, the wear rate of composite effectively decreases with the increases in the number of FSP (2, 4 and

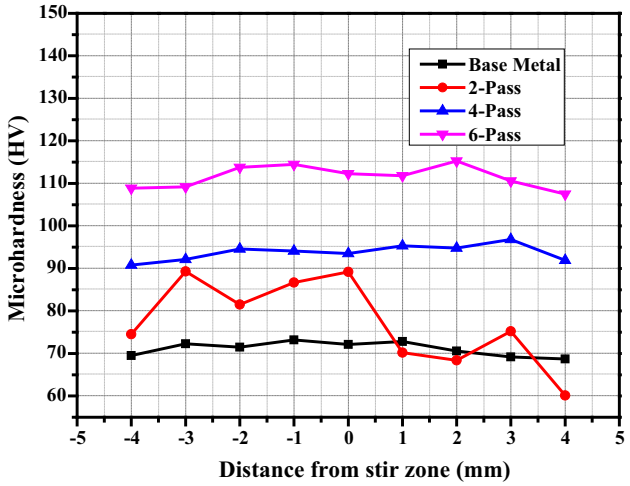

Fig. 6 Average microhardness value of base metal, 2-, 4- and 6-pass as-developed surface composite

6) passes. Increasing the number of processing passes delivers an equal scattering of the reinforcement particles ($ZrSiO_4$), decreases the surface cracks and pores and regulates and improves the microstructure. The formation of a strong, uniform mechanically passive layer over the surface of composite decreases the deterioration of wear resistance.

According to the studies, generation of low dynamism layer with low reciprocal coextensive site to matrix in fine-grained solid increases the corrosion–wear resistance as compared to that of coarse-grained film over surface [46]. Though, it has been described that as the FSP passes increase, the behavior of grain strictures reform from low grain energy to high grain energy boundaries/interfaces [47], which consequently reduces the veracity and chemical solidity of the developed passive layer. The wear (decomposition) rate of fabricated surface composite decreases as the FSP pass increases as shown in Fig. 8, and the wear rate of the 6-pass surface composite increases. These shows a good promise with the results of weight loss

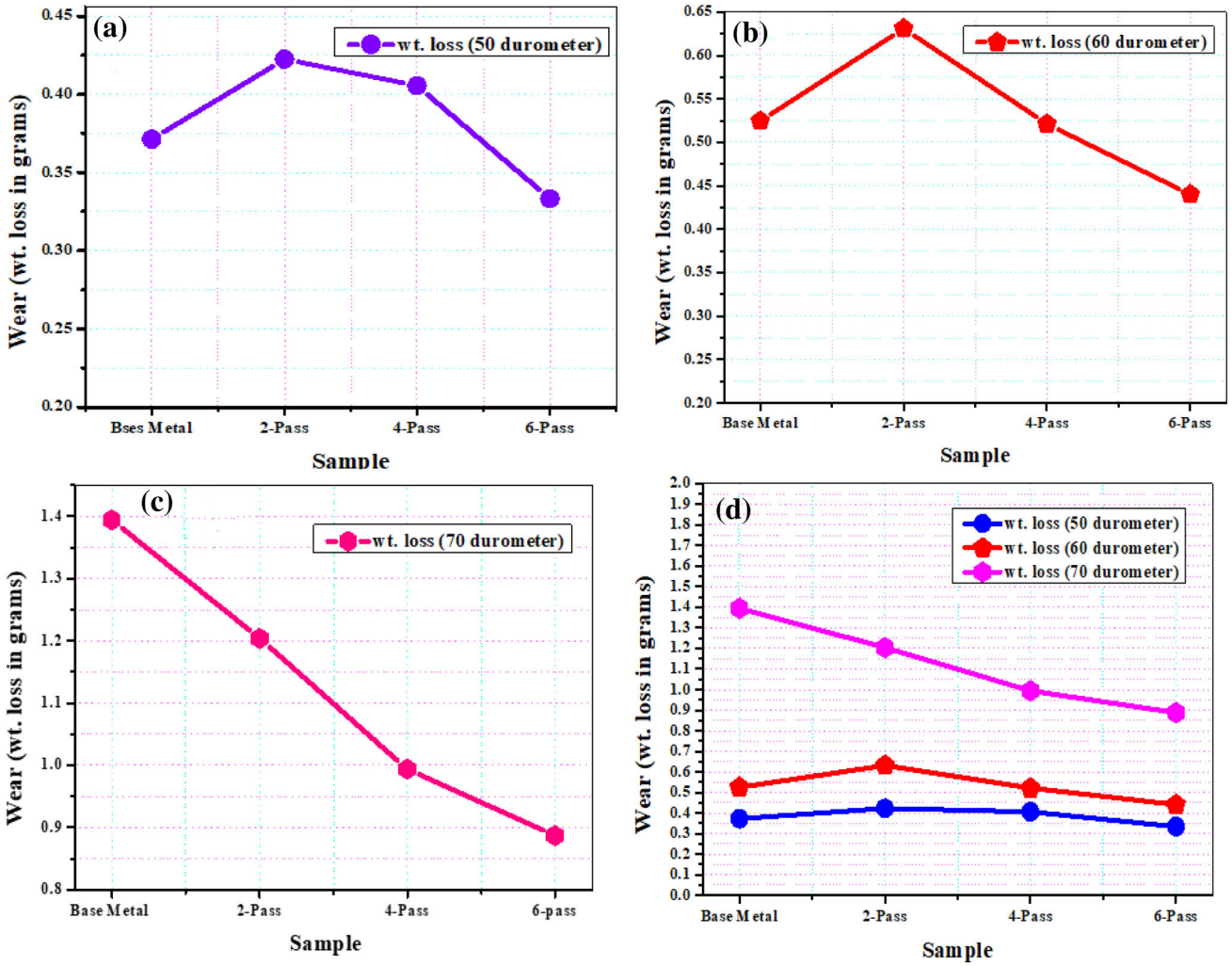

Fig. 7 Wear of materials **a** 50 durometer **b** 60 durometer **c** 70 durometer and **d** comparison of loss of materials at 50, 60 and 70 durometers

Table 3 Test parameters and wear of materials at different wheel hardness

Test parameters				
Specimen			Surface composites	
Load			2.5 kg	
Wheel speed			200 rpm	
Test duration			2000 Revolution	
Slurry			AFS 50/70 Quartz sand, slurry concentration 25%	
Wheel hardness (50 durometer)				
Run	Specimen weight in (gm)			Result
Run in test	Before test	After test	Wt. loss	Normalized Wt. loss (gm)
Base metal	43.45078	43.079523	0.37125	0.37125
2 pass	46.02442	45.60198	0.42244	0.42244
4 pass	47.63503	47.22955	0.40548	0.40548
6 pass	44.80755	44.44432	0.33323	0.33323
Wheel hardness (60 durometer)				
Base metal	44.25847	43.73369	0.52478	0.52478
2 pass	43.24230	42.61115	0.63115	0.63115
4 pass	43.31586	42.79483	0.52103	0.52103
6 pass	45.14273	44.70261	0.44012	0.44012
Wheel hardness (70 durometer)				
Base metal	46.25874	45.46416	0.79458	0.79458
2 pass	43.6960	42.4921	1.20386	1.20386
4 pass	43.15286	42.15905	0.99381	0.99381
6 pass	45.24273	44.35586	0.88687	0.88687

measurements. It is detected that the 4-pass composite reveals the superior ductility as compared to other composites and wear behavior while the 6-pass composite sample shows the superior tensile strength.

4 Conclusions

The zircon sand-reinforced aluminum (A4047) matrix composites with a significant control over the microstructural and grain features were fabricated through the FSP. The number of FSP passes could be measured as an effective process parameter to improve the performance of the modified composites. The fabricated composite was characterized through several properties (microstructural, tribological and mechanical properties). The processed composite showed better features of the effect on strength and microstructure of the composite. The number of friction stir processing passes and the developed composites promoted better grain refinement into the alloying element (A4047) and led to homogenous distribution of the zircon particles. Significant 6-pass FSP surface composite showed compactness into the stir zone. Similarly, the mechanical

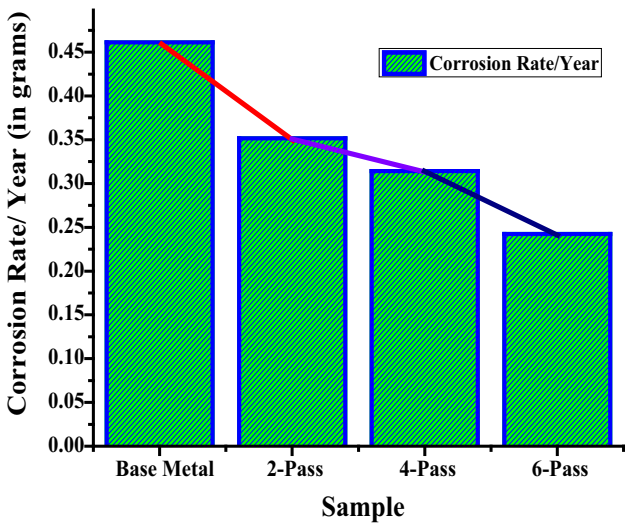

Fig. 8 Corrosion rate of base metal, 2-, 4- and 6-pass as-developed surface composite

properties (likely microhardness and tensile) of fabricated surface composites were improved by improving the number of FSP passes with existence of reinforcement (zircon) particles. The erosion–corrosion and abrasive wear resistance of the processed composites were significantly improved with increase in FSP pass. The increase in number of passes displayed abridged abrasion and corrosion and wear resistance of as-developed surface composite. It was observed that the experimental parameters would improve the strength and wear resistance of the Zircon/A4047 composites through friction stir processing.

Acknowledgements The authors gratefully acknowledge the financial support from National Institute of Technology, Mizoram. The authors also thank the characterization facility at laboratory department of MSME, Maulana Azad National Institute of Technology, Bhopal.

References

1. Isanaka S P, Karnati S, and Liou F, *Manuf Lett* **7** (2016) 11.
2. Kumaran S T, Kumar M U, Aravindan S, and Rajesh S, *J Mater Design Appl* **230** (2016) 484.
3. Pozdniakov A V, Zolotorevskiy V S, Barkov R Y, Lotfy A, and Bazlov A I, *J Alloys Compd* **664** (2016) 317.
4. Mazaheri Y, Karimzadeh F, and Enayati M H, *J Mater Process Technol* **211** (2011) 1614.
5. Sahraeinejad S, Izadi H, Haghshenas M, and Gerlich A P, *Mater Sci Eng A* **626** (2015) 505.
6. Kumar P V, Reddy G M, and Rao K S, *Def Technol* **11** (2015) 362.
7. Thankachan T, Prakash K S, and Kavimani V, *Mater Manuf Process* **33** (2018) 1681.
8. Zhang Z, Yang R, Guo Y, Chen G, Lei Y, Cheng Y, and Yue Y, *Mater Sci Eng A* **689** (2017) 411.
9. Mishra R S, Ma Z Y, and Charit I, *Mater Sci Eng A* **341** (2003) 307.
10. Mishra R S, Mahoney M W, McFadden S X, Mara N A, and Mukherjee A K, *Scr Mater* **42** (2000) 163.
11. Rahsepar M, and Jarahimoghadam H, *Mater Sci Eng A* **671** (2016) 214.
12. Barmouz M, Asadi P, Givi M K B, and Taherishargh M, *Mater Sci Eng A* **528** (2011) 1740.
13. Azizieh M, Goudarzi K, Pourmansouri R, Kafashan H, Balak Z, and Kim H S, *Trans Indian Inst Met* **71** (2018) 483.
14. Bauri R, Yadav D, Kumar C N S, and Balaji B, *Mater Sci Eng A* **620** (2015) 67.
15. Shafiei-Zarghani A, Kashani-Bozorg S F, and Zarei-Hanzaki A, *Mater Sci Eng A* **500** (2009) 84.
16. Shojaeefard M H, Akbari M, Khalkhali A, and Asadi P, *Mater Design Appl* **232** (2016) 637.
17. Zeidabadi S R H, and Daneshmanesh H, *Mater Sci Eng A* **702** (2017) 189.
18. Kishan V, Devaraju A, and Lakshmi K P, *Def Technol* **13** (2017) 16.
19. Hashemi S H, and Ashrafi A, *Trans IMF* **96** (2018) 52.
20. Shourgeshty M, Aliofkhazraei M, and Karimzadeh A, *Surf Eng* (2018) 10.1080/02670844.2018.1432172.
21. Tao X P, Zhang S, Wu C L, Zhang C H, Chen J, and Abdullah A O, *Surf Eng* **34** (2017) 316.
22. Abdollahi S H, Karimzadeh F, and Enayati M H, *J Alloys Compd* **623** (2015) 335.
23. Selvakumar S, Dinaharan I, Palanivel R, and Babu B G, *Mater Charact* **125** (2017) 317.
24. Patel S K, Kuriachen B, Kumar N, and Nateriya R, *Ceram Int* **44** (2018) 6432.
25. Kumar N, Shukla A, Kumar N, and Choudhary R N P, *Ceram Int* **45** (2019) 831.
26. Singh V P, Patel S K, Kumar N, and Kuriachen B, *J Sci Technol Weld Join* (2019). 10.1080/13621718.2019.1567031.
27. Kumar N, Shukla A, Kumar N, Choudhary R N P, and Kumar A, *RSC Adv* **8** (2018) 36950.
28. Kumar N, Shukla A, and Choudhary R N P, *Mater Int*, **28** (2018) 314.
29. Yuvaraj N, Aravindan S, and Vipin *Trans Indian Inst Met* **70** (2017) 1111.
30. Huang Y, Wang T, Guo W, Wan L, and Lv S, *Mater Design* **59** (2014) 274.
31. Jain V K S, Muhammed P M, Muthukumaran S, and Babu S P K, *Trans Indian Inst Met* **71** (2018) 1519.
32. Navazani M, and Dehghani K, *J Mater Process Technol* 229 (**2016**) 439.
33. Eskandari H, and Taheri R, *Procedia Mater Sci* **11** (2015) 503.
34. Ahmadifard S, Kazemi S, and Heidarpou A, *Mater Design Appl* **232** (2018) 287.
35. Janbozorgi M, Shamanian M, Sadeghian M, and Sepehrinia P, *Tran. Nonferrous Met Soc China* **27** (2017) 298.
36. Gangil N, Maheshwari S, and Siddiquee A N, *MaterManuf Process* **33** (2018) 805.
37. Akbari M, Shojaeefard M H, Asadi P, and Khalkhali A, *Mater Design Appl* (2017). 10.1177/1464420717702413.
38. Bhat U K, Udupa R K, Prakrathi S, and Huilgol P, *Trans Indian Inst Met* **69** (2016) 623.
39. Huan H S, Shuai Y, and Duo J, *Trans Indian Inst Met* **71** (2018) 985.
40. Rathee S, Maheshwari S, Siddiquee A N, and Srivastava M, *Trans Indian Inst Met* **70** (2017) 809.
41. Ge W, Lin F, and Guo C, *Mater Manuf Process* **33** (2018) 1708.
42. Barenji R V, Khojastehnezhad V M, Pourasl H H, and Rabiezadeh A, *J Compos Mater* **50** (2016) 1457.
43. Ramnath V, Elanchezhian C, Annamalai R M, Aravind S, Atreya T S A, Vignesh V, and Subramanian C, *Rev Adv Mater Sci* **38** (2014) 55.
44. Zhang W, Sun D, Han L, and Liu D, *Mater Design* **57** (2014) 186.
45. Reddy G M, and Rao K S, Trans Indian Inst Met **63** (2010) 793.
46. Alaneme K K, and Bodunrin M O, *J Miner Mater Charact Eng* **10** (2011) 1153.
47. Nelaturu P, Jana S, Mishra R S, Grant G, and Carlson B E, *Mater Sci Eng A* **716** (2018) 165.